

Sorption of Lead from Aqueous System using Palm Kernel Shell Biochar: Kinetic and Isotherm Studies

Soon Kong Yong¹, Sybialin Amin¹, Chia Chay Tay², Nur Firdaus Abdul Rashid³,
Nur Qursyna Boll Kassim⁴ and Vianney Siging^{1*}

¹Soil Assessment and Remediation Research Group, Faculty of Applied Sciences, Universiti Teknologi MARA, 40450 Shah Alam, Selangor, Malaysia

²Faculty of Applied Sciences, Universiti Teknologi MARA, 40450 Shah Alam, Selangor, Malaysia

³Faculty of Plantation and Agrotechnology, Universiti Teknologi MARA Perlis Branch, Arau Campus, 02600 Arau, Perlis, Malaysia

⁴Soil Conservation and Management Research Interest Group, Faculty of Plantation and Agrotechnology, UiTM Melaka Branch, Jasin Campus, 77300 Merlimau, Melaka, Malaysia

*Corresponding author (e-mail: vianneysiging@yahoo.com)

A cost-effective treatment for lead (Pb)-contaminated wastewater has been a challenge due to the high consumption of costly chemicals. Palm kernel shell (PKS) has been used as a solid fuel for boilers. An incomplete combustion produces a by-product called PKS biochar that can be used as a sorbent for the removal of Pb from wastewater. The objectives of this study are to determine the optimized sorption parameters and to study the Pb sorption mechanism of PKS biochar using non-linear kinetics and isotherm models. The maximum Pb removal was achieved at a PKS biochar dosage of 1.25 g/L, and at pH 5. The sorption data were best described by the Langmuir isotherm model (R^2 : 0.9478) and the pseudo-second order model (R^2 : 0.9317). The Langmuir maximum Pb sorption capacity of PKS biochar was 7.48 mg/g. The decrease of cation exchange capacity (CEC) and intensity of the -OH band in Fourier transform infrared (FTIR) spectra indicate a net loss of negative-charge oxygen functional groups via decarboxylation and decarbonylation. The slightly increased iodine number and BET surface area corroborated with proximate analysis, showing that pyrolysis at 500 °C did not eliminate volatile matter from the pore of PKS biochar. The sorption process may have involved the formation of the Pb monolayer on the surface of PKS biochar, and indicate the rate-limiting step of the Pb sorption process is the formation of strong chemical bonds.

Keywords: Charcoal; black carbon; biochar; activated carbon; lead

Received: November 2022; Accepted: January 2023

Heavy metal pollution in water resources has become a major concern due to its adverse impact on public health and the environment. Lead (Pb) is one of the heavy metals commonly detected in trace amounts in contaminated waters. The sources of anthropogenic Pb include solder, car batteries, and leaded ammunition [1]. The trace amount of Pb in the environment may become a serious threat to human health due to possible bioaccumulation and biomagnification in the food chain [2]. Ingestion of Pb-contaminated food may adversely affect the central and peripheral nervous system [3]. Children, in particular, are more susceptible to the health impact of Pb poisoning [4]. Hence, the removal of Pb is a great priority to ensure the safety of food and water resources and the well-being of the public.

Currently, the precipitation method is the most common method to remove Pb from wastewater [5]. However, the removal efficiency is impacted by a low pH and the presence of background ions [6]. Furthermore, large amounts of chemicals (i.e., phosphate salts

and limestone) are required and are not economically feasible [7]. Other technologies such as membrane filtration, ion exchange, and electrocoagulation are effective in removing Pb but are relatively expensive due to high energy input requirements [8]. A cost-effective approach for removing trace Pb in water is sorption using naturally available materials such as agricultural waste and its derivatives [9].

Malaysia produces a large amount of agricultural solid waste, particularly, from its palm oil industry. Palm kernel shell (PKS) has been recovered due to its high calorific value and is used as a solid fuel for boilers [10]. A possible lack of oxygen supply during combustion produces a carbon-rich, alkaline material called biochar [11]. If produced at a high pyrolysis temperature, biochar can possess a high surface area and alkalinity that is effective in removing Pb from wastewater. Furthermore, the carbon in biochar can withstand degradation and hold the adsorbed Pb [12]. Despite the great potential of PKS as feedstock for the production of biochar sorbent, most reports focused on

the immobilization of Pb in soil [13]. The sorption of Pb using PKS has just recently been reported [14]. In this study, PKS biochar was characterized and the sorption performance for the removal of Pb in an aqueous system was evaluated. Several sorption parameters (i.e., sorbent dosage, and solution pH) were optimized to determine the highest Pb removal by PKS biochar. The maximum Pb sorption capacity (mg/g) and its removal mechanism of PKS biochar were investigated using isotherm models (i.e., Langmuir and Freundlich) and kinetic models (i.e., pseudo-second order and pseudo-first order).

EXPERIMENTAL

Preparation of PKS Biochar

The as-received PKS was collected from Endau Palm Oil Mill Sdn Bhd at Petaling Jaya, Selangor. Raw PKS was first rinsed with distilled water and then oven-dried at 110°C for 12 hours. The dried PKS was pulverized and sieved to a fine and uniform particle with a diameter of <2 mm. As shown in Figure 1, PKS biochar was produced by pyrolysis of PKS at a peak temperature of 500°C for 45 min before being quenched and flushed with distilled water until pH 8. The resulting

PKS biochar was oven-dried at 105°C for 12 hours and was then sent for physicochemical analyses.

Characterization Methods

The proximate analysis for raw PKS and PKS biochar was conducted by thermogravimetric analysis [15]. The fixed carbon content was calculated by the summation of percentages of moisture, ash, and volatile matter subtracted from 100 [16]. Surface functional groups of PKS and PKS biochar were analyzed using FTIR spectroscopy (Perkin Elmer, Spectrum One). Sample pellets were prepared by mixing and pressing about 1 mg of the pulverized PKS and PKS biochar with 100 mg potassium bromide. The FTIR spectrum was collected at the wavenumber range of 4000 cm⁻¹ to 450 cm⁻¹ with 64 scans and a resolution of 4 cm⁻¹. For determining the surface area of raw PKS and PKS biochar, the iodine number [17] and BET (N₂) methods [18] were adopted. Cation exchange capacity was also determined using the sodium acetate method [19]. The surface morphology of the raw PKS biochar was studied using scanning electron microscopy (SEM) (Hitachi TM3030plus). Samples were sputter-coated with carbon and mounted on the copper stub using double-stick carbon tape.

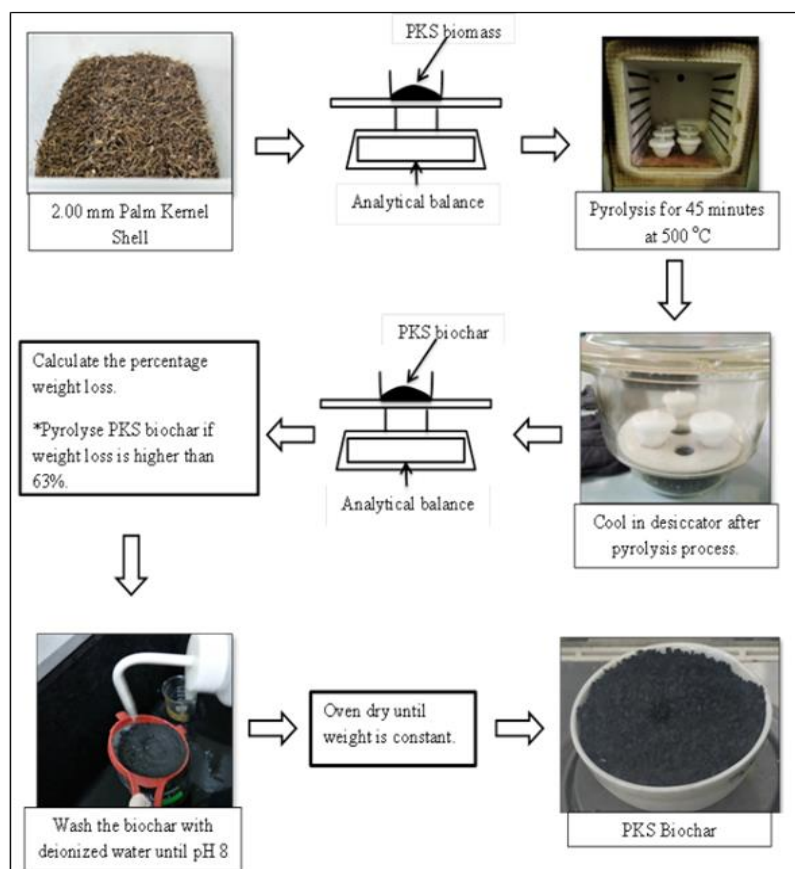


Figure 1. Preparation of PKS biochar

Batch Sorption Experiment

Wastewater with a pre-determined concentration of Pb was artificially prepared by diluting the stock lead nitrate solution (Pb concentration: 1000 mg/L) with deionized water. The Pb removal of PKS biochar was conducted by varying the value of sorbent dosage (i.e., 0.01 g, 0.05 g, 0.10 g, 0.15 g, and 0.20 g), and solution pH (i.e., 2, 3, 4, 5, 6). The batch sorption experiments were conducted in a 50 mL centrifuged tube and the desired solution pH was obtained by adding 0.1 M NaOH or 0.1 M HNO₃. The optimization of sorbent dosage was conducted by mixing various amounts of PKS biochar (i.e., 0.01 g, 0.05 g, 0.10 g, 0.15 g, and 0.20 g) with 40 mL of 70 mg/L Pb solution with a rotator at 70 rpm for 2.5 hours. Once the sorption process is complete, PKS biochar was separated by centrifugation and filtered using Whatman filter paper No.4. The supernatants containing residual Pb were collected, and preserved with one drop of concentrated nitric acid. The optimization for solution pH was conducted at pH 2, 3, 4, 5, and 6 using 0.05 g of PKS biochar. The solution pH was adjusted with 0.1 M NaOH and 0.1 M HNO₃ solutions. The sorption kinetic experiment was conducted using the optimized sorbent dosage and solution pH. The mixture of PKS biochar and Pb solution (70 mg/L) was rotated at 70 rpm at various contact times of 15, 30, 60, 90, 120, and 150 minutes. The content in the centrifuge tubes was agitated using a rotator for the required contact time. The batch sorption isotherm experiment was conducted using aqueous solutions with various initial Pb concentrations. Both the initial and the residual concentration of Pb were analyzed with the atomic absorption spectrophotometer (Perkin Elmer Analyst 400 flame ionization detector, FID). The Pb percentage removal (% Removal), was calculated by using Eq (1):

$$\% \text{ Removal} = \frac{(C_0 - C_e)100}{C_0} \quad \text{Eq (1)}$$

where, % Removal is percentage of Pb removal; C₀ is initial lead concentrations (mg/L); C_e is residual Pb concentrations, (mg/L).

The sorption capacity of Pb was calculated with Eq (2):

$$q_e = \frac{(C_0 - C_e)V}{m} \quad \text{Eq (2)}$$

where, q_e is sorption capacity (mg/g); C₀ is initial Pb concentrations (mg/L); C_e is residual Pb concentrations (mg/L); m is mass of the PKS biochar (g)

Sorption Isotherm

The non-linear Langmuir isotherm model used in this study was shown in Eq (3)

$$q_e = \frac{Q_{max}bC_e}{1 + bC_e} \quad \text{Eq (3)}$$

where, q_{max} is maximum adsorption capacity (mg/g); b is Pb binding affinity (L/mg)

The separation factor R_L was calculated with Eq (4) to predict the favorability of the sorption system:

$$R_L = \frac{1}{1 + bC_e} \quad \text{Eq (4)}$$

where, C_e is residual Pb concentration (mg/L); b is the affinity constant of the Langmuir isotherm model (mL/mg). The sorption process, R_L was described as:

R_L > 1; unfavourable, R_L = 1; Linear, 0 < R_L < 1; favourable and R_L = 0; irreversible.

Meanwhile, the Freundlich isotherm model was given in Eq 5:

$$q_e = K_F C_e^{1/n} \quad \text{Eq (5)}$$

where, q_e is adsorbed weight of Pb per unit weight of PKS biochar; K_F and n: Freundlich empirical constants (L/g); C_e is the ion equilibrium concentration.

Sorption Kinetics

The non-linear pseudo-first order model (Eq 6) and pseudo-second order model (Eq 7) are as follows:

$$q_t = q_e(1 - \exp(-k_1t)) \quad \text{Eq (6)}$$

$$q_t = \frac{q_e^2 k_2 t}{1 + q_e k_2 t} \quad \text{Eq (7)}$$

where, q_e is the amount of Pb adsorbed at equilibrium (mg/g); q_t is the sorption capacities at equilibrium (mg/g) at any time of reaction; t is contact time (mins); k₁ (min⁻¹) and k₂ are rate constants of pseudo-first order and pseudo-second order models, respectively. The analyses of sorption kinetic and isotherm models were conducted using Sigma Plot software.

RESULTS AND DISCUSSION

Physico-chemical Characterization

Figure 2 shows the thermogram for raw PKS and PKS biochar. The yield of PKS biochar was 35 ± 7 % dry basis (d.b.). Approximately 6.44% moisture was removed from PKS during the first heating step (i.e., 30-105°C). The second heating step that occurred between 105-800°C decomposed biomass constituents into the volatile matter and form new aromatic carbon structures [16]. The moisture content, volatile matter, fixed carbon, and ash content for raw PKS and PKS biochar are shown in Table 1. The content of volatile matter content for raw PKS (60.1 % d.b.) is comparable to values reported in the literature (69.9 % d.b.) [20]. The volatile matter for PKS biochar is 17.5 % d.b., this indicates a strong adherence to the volatile constituents

from palm oil despite being pyrolyzed at 500°C. The fixed carbon content of PKS biochar was higher (i.e., 65.1) compared to raw PKS (13.9 % d.b.). The increased carbon content in the PKS biochar was due to the loss of oxygen functional groups via decarboxylation and decarbonylation during the pyrolysis of PKS [20]. In the fourth and final step, oxygenated combustion at 850°C converted all organic matter to carbon dioxide, leaving only ash at the end of the process. Figure 2 shows that raw PKS has a higher ash content (26.0 % d.b.) than PKS biochar (17.4 %). The extensive rinsing of PKS biochar during its preparation may have caused the loss of ash content.

Figure 3 and Table 2 summarise all the functional groups present in raw PKS and PKS biochar. A broad and strong band at around 3300–3400 cm^{-1} was

observed in the FTIR spectrum for raw PKS. However, this band almost disappeared for PKS biochar. This band is attributed to the O-H stretching vibration for hydroxyl groups (i.e. phenolic, aliphatic hydroxyl) and carboxylic group [20]. A strong C-O stretch band at around 1000-1300 cm^{-1} was observed in the FTIR spectrum of raw PKS, indicating a high content of oxygen functional groups present in cellulose, lignin, and hemicellulose [20]. This band is weaker in the FTIR spectrum of PKS biochar, suggesting that the decomposition of biomass constituents occurred. There is a strong and broad band of C=C stretching at 1510-1650 cm^{-1} in the FTIR spectrum of PKS biochar, proving the presence of the aromatic ring group [21]. Moreover, the band around 1570-1515 cm^{-1} was due to the N-H bending of the amide group.

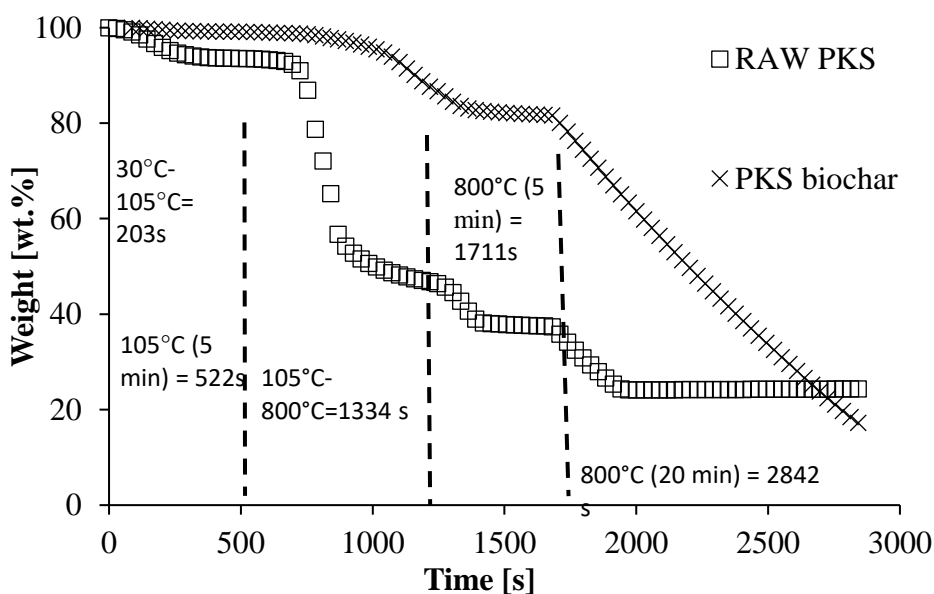


Figure 2. Thermogram for raw PKS (square) and PKS biochar (cross)

Table 1. Proximate analysis for raw PKS and PKS biochar

	Raw PKS	PKS Biochar
moisture content (%)	6.44	0.86
volatile matter (%)	60.1	17.5
fixed carbon (%)	13.9	65.1
ash content (%)	26	17.4

*the analysis is based on dry basis (d.b.)

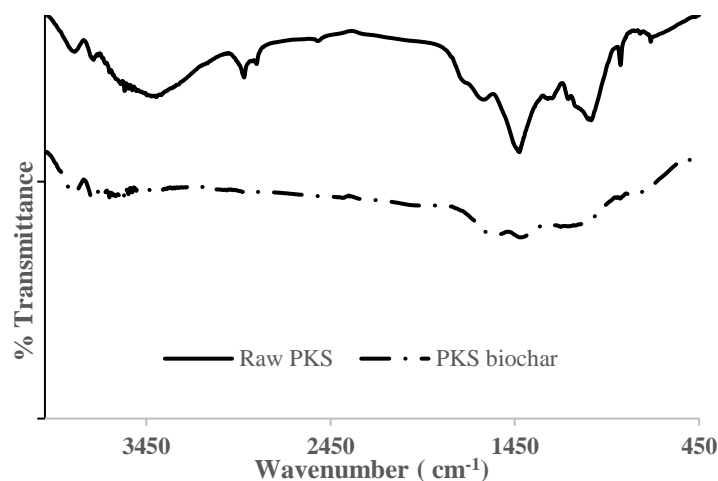


Figure 3. FTIR spectra of raw PKS and PKS biochar

Table 2. FTIR vibration bands in raw PKS and PKS biochar

Vibration bands	Wavenumber (cm ⁻¹)	
	Raw PKS	PKS biochar
O-H stretching	3394	-
C-O-H bending	1424	1421
C=C stretching	-	1537
C-O-C stretching	1031	1197
N-H bending	-	1537

Table 3 shows CEC, iodine number, and BET surface area for raw PKS and PKS biochar. The CEC value for raw PKS was higher than that of PKS biochar. Raw PKS had several oxygen functional groups (i.e., hydroxyl and carboxyl) that contribute to a high CEC value. The PKS biochar has lost oxygen functional groups through decarboxylation and decarbonylation reactions that contributed to its lower CEC value. The iodine number for PKS biochar was higher than that of raw PKS. PKS biochar may possess a higher content of micropores for sorbing more iodine on its surface [22]. The BET surface area for PKS biochar was lower than the values reported in the literature. For example, [23] pyrolyzed PKS at 500°C for 1 hr and obtained a BET surface area of 84 m²/g while [24] reported a value of 191 m²/g under similar pyrolysis temperature

and holding time. [25] gasified PKS at 725 ± 75°C and reported a BET surface area of 23.7 m²/g. It is noteworthy that the volatile matter for PKS biochar (17.5 %) is also higher than that (12.3 %) reported by [24]. The presence of excess volatile matter in the PKS biochar may indicate the presence of tar that blocks the micropores causing the low BET surface area.

Scanning Electron Micrography

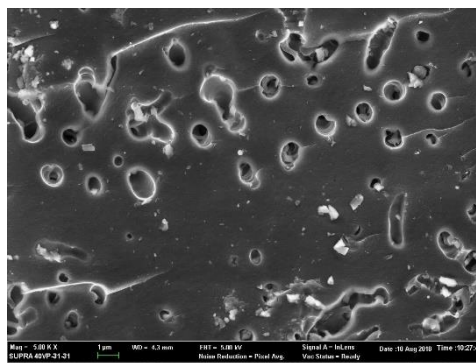
Figure 4 shows SEM images for raw PKS [26] and PKS biochar. Raw PKS has no apparent porous structure. A small area on the surface of PKS biochar was porous. This is consistent with the finding in the specific surface area analysis, whereby the higher amount of macropore on the outer sphere of PKS was the result of the pyrolysis of PKS.

Table 3. Cation exchange capacity (CEC), iodine number, and BET surface area for raw PKS and PKS biochar

Type of sample	CEC (cmol/kg)	Iodine number (mg/g)	BET surface area (m ² /g)
Raw PKS	10.8	61.5	N/D
PKS biochar	2.33	65.6	1.44



(i)



(ii)

Figure 4. SEM images for (i) raw PKS [26], and (ii) PKS biochar

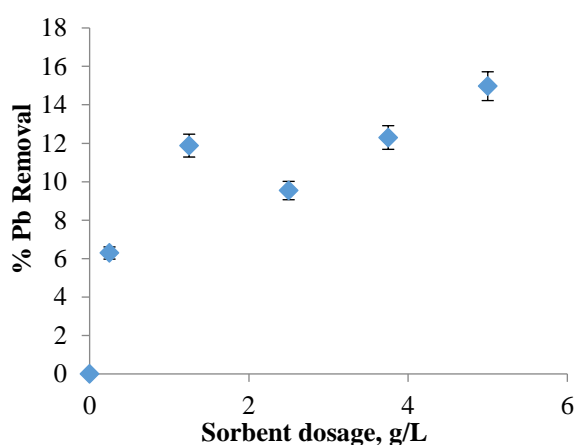


Figure 5. The percentage removal of Pb (% d.b.) as a function of sorbent dosage (g/L) of PKS biochar (Solution pH 5, contact time 2.5 hours, initial Pb concentration 70 mg/L, agitation 70 rpm, temperature 25°C)

Optimization of the Sorption Parameter

Figure 5 shows the % Pb removal at various sorbent dosages of PKS biochar. The % Pb removal increased with higher sorbent dosage until 1.25g/L. Further increase in sorbent dosage did not significantly improve % Pb removal beyond 11.88% d.b., at which point the optimum sorbent dosage for PKS biochar is obtained.

The increasing Pb removal can be due to the availability of active sites on the surface of the sorbent for bonding with Pb [27]. The amount of Pb adsorbed by adsorbent and the amount of ions remaining in the solution remains almost constant even with adding the dose of adsorbent. The Pb percentage removal for PKS biochar was lower compared to those reported in the literature. The large particle size of PKS biochar (<2.0 mm) may

possess a low BET surface area and low availability of active sites may have limited sorption of Pb and contribute to a lower than expected percent Pb removal.

Effect of pH

Figure 6 illustrates the percent Pb removal at various initial pH of the Pb solution. The percent Pb removal increased until 10.33% d.b. at a pH of 6.07. The pH 5 was selected as an optimum value because at pH 6, Pb in the solution may be precipitated [28]. The low percent Pb removal at acidic condition was explained by the competition between Pb^{2+} and H^+ ions for the active sites on the sorbent surface [29]. A high concentration of H^+ may cause protonation to give a positive-charge surface on PKS biochar and repel Pb^{2+} ions, thus, further decreasing the binding of Pb to the active sites [30].

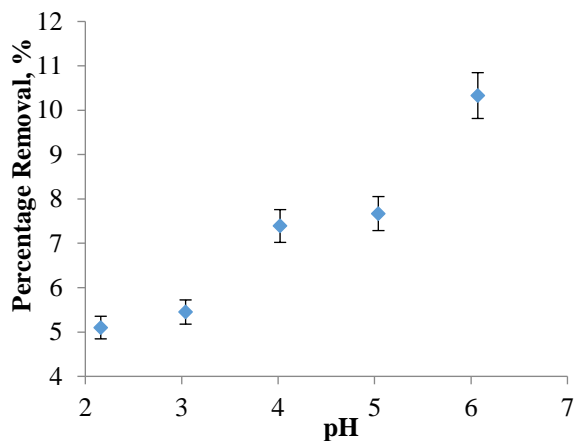


Figure 6. Percentage Pb removal by PKS Biochar at various solution pH (Sorbent dosage (1.25 g/L), initial Pb concentration (70 mg/L), contact time 2.5 hours, agitation 70 rpm, temperature 25°C)

Sorption Kinetic

The Pb percentage removal increased with the increasing contact time and became plateaued after the 60th minute. Figure 7 shows the regression plots of nonlinear pseudo-first order and pseudo-second order kinetic models. Table 4 shows the sorption rate constants. Sorption data is well fitted to the pseudo-

first order (R^2 : 0.931) and pseudo-second order kinetic models (R^2 : 0.933). The q_e value (4.52 mg/g) from the pseudo-second order model matched the experimental q_e value (4.37 mg/g). A high fitness of the sorption data to the pseudo-second order kinetic model indicates the rate-limiting step of the chemical sorption process [31], possibly, bonding between Pb and the active site on the surface of PKS biochar had taken place.

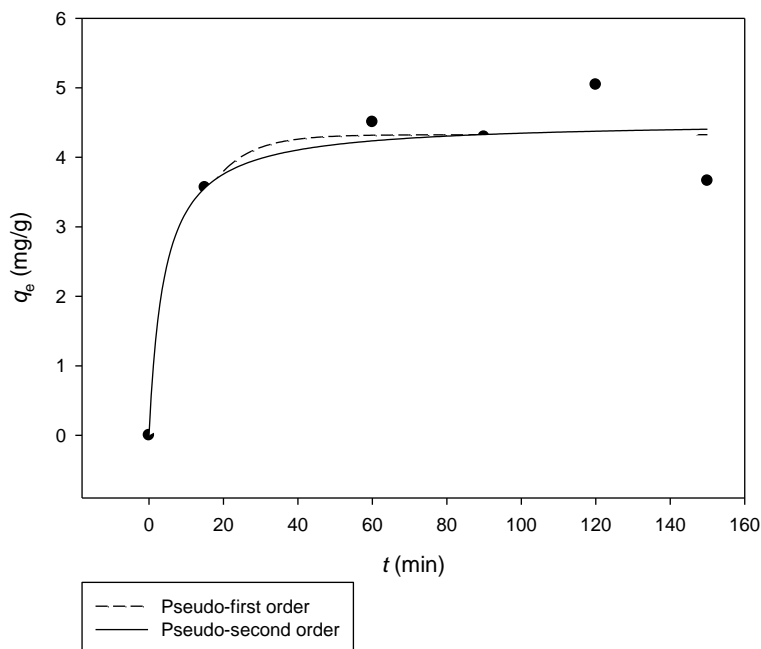


Figure 7. The regressions plots of nonlinear pseudo-first order and pseudo-second order kinetic models for the sorption of Pb by PKS biochar

Table 4. Pseudo-first order and pseudo-second order kinetic parameters for sorption of Pb by PKS biochar

Kinetic model	Parameter	Value
Pseudo-first order	q_e (mg/g)	4.33
	k_1 (min ⁻¹)	0.105
	R^2	0.931
Pseudo-second order	q_e (mg/g)	4.52
	k_2 (g mg ⁻¹ min ⁻¹)	0.0543
	R^2	0.933

Sorption Isotherm

Figure 8 shows the nonlinear regression plots of non-linear Langmuir and Freundlich isotherm models for the sorption of Pb by PKS biochar. The sorption isotherm parameters were summarized in Table 5. The Langmuir model has a higher regression coefficient (R^2 : 0.948), and is better than the Freundlich model (R^2 : 0.936) in describing the sorption isotherms. The Langmuir maximum Pb sorption capacity (q_{max}) of PKS biochar was 7.47 mg/g. The separation factor

(R_L) value was 0.938. This indicates that the sorption of Pb by PKS biochar is a favorable process. A high fitness of the sorption data to the Langmuir isotherm model reflects a strong monolayer sorption of Pb on the surface of PKS biochar. Furthermore, the n value from the Freundlich models was 1.86 (Table 5). If the n value is > 1 , the physical sorption process between Pb and PKS biochar is dominant. The situation in which $n > 1$ was common and due to a distribution of surface areas or any factor that causes a decrease in Pb-PKS biochar interaction with increasing surface density [32].

Table 5. Langmuir and Freundlich isotherm models parameters for sorption of Pb by PKS biochar

Model	Parameter	Value
Langmuir	K_L (L/mg)	0.0154
	q_{max} (mg/g)	7.47
	R^2	0.948
	R_L	0.938
Freundlich	K_F (mg/g)	0.392
	n	1.86
	R^2	0.936

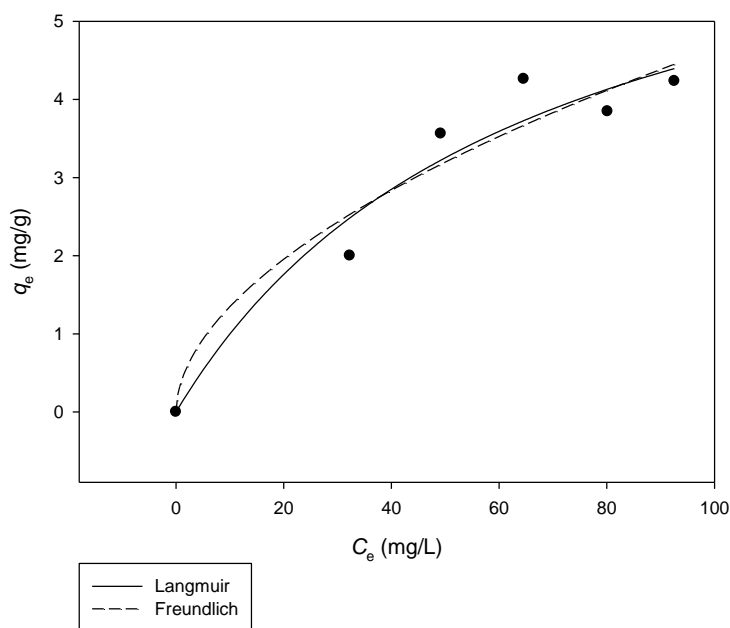


Figure 8. Plots of q_e as a function of C_e fitted with Langmuir and Freundlich isotherm models

CONCLUSION

The high fitness of sorption data to the Langmuir isotherm model and pseudo-second kinetic model shows that the sorption process occurred via the formation of a Pb monolayer and is attached to the PKS biochar surface via a chemical bond. Based on this study, PKS biochar has shown potential as a sorbent for removing Pb from wastewater. However, the maximum sorption capacity was lower than those reported in the literature possibly because PKS biochar is relatively larger in particle diameter and volatile matter persists in the pores of PKS biochar. The number of active sites for binding Pb may have been increased if a higher peak pyrolysis temperature and a finer PKS feedstock is employed during the preparation of PKS biochar. This proves that producing a sorbent from dense and oily feedstock such as PKS and is good enough for the sorption of cationic elements such as Pb^{2+} is still a challenge. Nonetheless, unwashed PKS biochar still possesses great potential for removing Pb due to the high content of alkaline ash. More studies on PKS biochar should be conducted especially on those modified with catalytic and magnetic properties to further enhance its effectiveness and recoverability.

ACKNOWLEDGEMENTS

The authors gratefully acknowledge the financial assistance from the Research Management Centre, Universiti Teknologi MARA in providing the Special Research Grant (Geran Penyelidikan Khas) 600-RMC/GPK 5/3 (093/2020) and Professor Robert Thomas Bachmann from the Malaysian Institute of Chemical and Bioengineering Technology, Universiti Kuala Lumpur for providing technical assistance in preparing and analyzing PKS biochar.

REFERENCES

1. Yong, S. K., Zin, S. N. M. and Ariff, M. J. M. (2016) Effects of rain pH, soil organic matter, cation exchange capacity and total lead content in shooting range soil on the concentration of lead in leachate. *Malaysian Journal of Analytical Sciences*, **20**, 1066–1072.
2. Kumar, A., Kumar, A., Cabral-Pinto, M. M. S., Chaturvedi, A. K., Shabnam, A. A., Subrahmanyam, G., Mondal, R., Gupta, D. K., Malyan, S. K., Kumar, S. S., Khan, S. A. and Yadav, K. K. (2020) Lead Toxicity: Health Hazards, Influence on Food Chain, and Sustainable Remediation Approaches. *Int J Environ Res Public Health*, **17**, 2179.
3. Collin, M. S., Venkatraman, S. K., Vijayakumar, N., Kanimozhi, V., Arbaaz, S. M., Stacey, R. G. S., Anusha, J., Choudhary, R., Lvov, V., Tovar, G. I., Senatov, F., Koppala, S. and Swamiappan, S. (2022) Bioaccumulation of lead (Pb) and its effects on human: A review. *Journal of Hazardous Materials Advances*, **7**, 100094.
4. Hauptman, M., Bruccoleri, R. and Woolf, A. D. (2017) An Update on Childhood Lead Poisoning. *Clin Pediatr Emerg Med*, **18**, 181–192.
5. Chowdhury, I. R., Chowdhury, S., Mazumder, M. A. J. and Al-Ahmed, A. (2022) Removal of lead ions (Pb^{2+}) from water and wastewater: a review on the low-cost adsorbents. *Applied Water Science*, **12**, 185.
6. Di Lorenzo, F., Steiner, K. and Churakov, S. V. (2021) The Effect of pH, Ionic Strength and the Presence of PbII on the Formation of Calcium Carbonate from Homogenous Alkaline Solutions at Room Temperature. *Minerals*, **11**, 783.
7. Qasem, N. A. A., Mohammed, R. H. and Lawal, D. U. (2021) Removal of heavy metal ions from wastewater: a comprehensive and critical review. *npj Clean Water*, **4**, 36.
8. Plappally, A. K. and Lienhard V, J. H. (2012) Energy requirements for water production, treatment, end use, reclamation, and disposal. *Renewable and Sustainable Energy Reviews*, **16**, 4818–4848.
9. Yong, S. K., Leyom, J., Tay, C. C. and Talib, S. A. (2018) Sorption of lead from aqueous system using cocoa pod husk biochar: Kinetic and isotherm studies. *International Journal of Engineering & Technology*, **7**, 241–244.
10. Umar, H. A., Sulaiman, S. A., Meor Said, M. A. and Ahmad, R. K. (2020) Palm Kernel Shell as Potential Fuel for Syngas Production, in *Advances in Manufacturing Engineering: Lecture Notes in Mechanical Engineering*, eds. S. S. Emamian, M. Awang, & F. Yusof, Springer Nature: Singapore.
11. Kong, S. H., Loh, S. K., Bachmann, R. T., Choo, Y. M., Salimon, J. and Rahim, S. A. (2013) Production and physico-chemical characterization of biochar from palm kernel shell. *AIP Conference Proceedings*, **1571**, 749–752.
12. Hansson, A., Haikola, S., Fridahl, M., Yanda, P., Mabhuye, E. and Pauline, N. (2021) Biochar as multi-purpose sustainable technology: experiences from projects in Tanzania. *Environment, Development and Sustainability*, **23**, 5182–5214.
13. Anegebe, B., Okuo, J., Ewekay, E. and Ogbeifun, D. (2014) Fractionation of lead-acid battery soil amended with Biochar. *Bayero Journal of Pure and Applied Sciences*, **7**, 36–43.

- 126 Soon Kong Yong, Sybilin Amin, Chia Chay Tay, Nur Firdaus Abdul Rashid, Nur Qursyna Boll Kassim and Vianney Siging Sorption of Lead from Aqueous System using Palm Kernel Shell Biochar: Kinetic and Isotherm Studies
14. Baby, R., Saifullah, B. and Hussein, M. Z. (2019) Palm Kernel Shell as an effective adsorbent for the treatment of heavy metal contaminated water. *Scientific Reports*, **9**, 18955.
15. Mayoral, M. C., Izquierdo, M. T., Andrés, J. M. and Rubio, B. (2001) Different approaches to proximate analysis by thermogravimetry analysis. *Thermochemica Acta*, **370**, 91–97.
16. Dewayanto, N., Azman, A. N., Ahmad, N. A. and Mohd Shah, M. S. H. (2016) Study of thermal degradation of biomass wastes generated from palm oil milling plant. *CHEMICA Jurnal Teknik Kimia*, **3**, 31–37.
17. ASTM D4607-94 (1999) Standard test method for determination of iodine number of activated carbon, American Society for Testing and Materials, PA 19428.
18. Brunauer, S., Emmett, P. H. and Teller, E. (1938) Adsorption of Gases in Multimolecular Layers. *Journal of the American Chemical Society*, **60**, 309–319.
19. USEPA Method 9081 (1986) Cation Exchange Capacity of Soils (Sodium Acetate), United States Environmental Protection Agency, DC 20004.
20. Asadieraghi, M. and Wan Daud, W. M. A. (2014) Characterization of lignocellulosic biomass thermal degradation and physicochemical structure: Effects of demineralization by diverse acid solutions. *Energy Conversion and Management*, **82**, 71–82.
21. Wang, P., Zhang, J., Shao, Q. and Wang, G. (2018) Physicochemical properties evolution of chars from palm kernel shell pyrolysis. *Journal of Thermal Analysis and Calorimetry*, **133**, 1271–1280.
22. Danish, M., Hashim, R., Ibrahim, M. M., Rafatullah, M., Ahmad, T. and Sulaiman, O. (2011) Characterization of Acacia mangium wood based activated carbons prepared in the presence of basic activating agents. *BioResources*, **6**, 3019–3033.
23. Guo, J. and Lua, A. C. (1998) Characterization of chars pyrolyzed from oil palm stones for the preparation of activated carbons. *Journal of Analytical and Applied Pyrolysis*, **46**, 113–125.
24. Lee, Y., Park, J., Ryu, C., Gang, K. S., Yang, W., Park, Y. -K., Jung, J. and Hyun, S. (2013) Comparison of biochar properties from biomass residues produced by slow pyrolysis at 500°C. *Bioresource Technology*, **148**, 196–201.
25. Mahmood, W., Ariffin, M., Harun, Z., Ishak, N., Ghani, J. A. and Ab Rahman, M. N. (2015) Characterisation and potential use of biochar from gasified oil palm wastes. *Journal of Engineering Science and Technology*, **10**, 45–54.
26. Ramli, A. and Mohd Ghazi, R. (2020) Removal of Oil and Grease in Wastewater using Palm Kernel Shell Activated Carbon. *IOP Conference Series Earth and Environmental Science*, **549**, 012064.
27. Moyo, M., Chikazaza, L., Nyamunda, B. C. and Guyo, U. (2013) Adsorption Batch Studies on the Removal of Pb(II) Using Maize Tassel Based Activated Carbon. *Journal of Chemistry*, **2013**, 508934.
28. Li, X., Azimzadeh, B., Martinez, C. E. and McBride, M. B. (2021) Pb Mineral Precipitation in Solutions of Sulfate, Carbonate and Phosphate: Measured and Modeled Pb Solubility and Pb²⁺ Activity. *Minerals*, **11**, 620.
29. Chaouch, N., Ouahrani, M. R. and Laouini, S. E. (2014) Adsorption of Lead (II) from aqueous solutions onto activated carbon prepared from Algerian dates stones of *Phoenix dactylifera*.L (Ghars variety) by H₃PO₄ activation. *Oriental Journal of Chemistry*, **30**, 1317–1322.
30. Iyagba, E. and Opete, O. (2009) Removal of chromium and lead from drill cuttings using activated palm kernel shell and husk. *African Journal of Environmental Science and Technology*, **3**, 171–179.
31. Ho, Y. -S. (2014) Using of “pseudo-second-order model” in adsorption. *Environmental Science and Pollution Research*, **21**, 7234–7235.
32. Desta, M. B. (2013) Batch Sorption Experiments: Langmuir and Freundlich Isotherm Studies for the Adsorption of Textile Metal Ions onto Teff Straw (*Eragrostis tef*) Agricultural Waste. *Journal of Thermodynamics*, **2013**, 375830.